

# The synchronized force impact measurement and visualization of single cavitation bubble generated with LIB

D. Jasikova, M. Muller, M. Kotek and V. Kopecky

**Abstract**—In this paper we present the results of the synchronized investigation of the single cavitation bubble behavior. The cavitation bubble is generated with Laser Induced Breakdown (LIB) technique that is based on single laser shot that is synchronized with a high speed shadowgraphy visualization and the pressure force measurement. The bubble dynamics response in the field of fluid can be detected acoustically by PVDF needle hydrophones or optically by high speed CCD cameras working on frequencies up to 180 kHz. Here we present two PVDF film signals corresponding to two bubble wall distances and we are following the run of the first peak in the signal, which corresponds to the interaction between the wall and shock wave, which is radiated at the bubble initiation due to rapid plasma expansion. The main goal of this research was to set the optical setup for the laser induced breakdown and to create the calibration relation curve for the bubble size dependence on the input energy of the laser beam.

This calibration curve was related to the collapse time of the cavitation bubble to estimate the lifespan of each bubble. This information was the entry condition for the setup of the visualization technique.

**Keywords**— Laser induced breakdown, Shadowgraphy, Cavitation bubble, Bubble wall interaction.

## I. INTRODUCTION

THE cavitation can be defined as a collection of effects connected to the origin, activities and collapse of macroscopic bubbles in liquid. In real applications cavitation bubbles are usually not separated. The bubbles create structures which act collectively, however the essential elements of these structures are the individual bubbles.

The understanding of its dynamics and impact to the surroundings represents the key in the understanding of the cavitation phenomena in its complexity.

The bubbles can be generated by several physically different mechanisms. The most obvious in nature is the hydrodynamics cavitation, where the bubbles are produced due to local pressure decrease caused by the flow acceleration in vicinity of obstacles. Acoustic cavitation is produced by

The results of this project LO1201 were obtained through the financial support of the Ministry of Education, Youth and Sports in the framework of the targeted support of the “National Programme for Sustainability I”

D. Jasikova is with the Institute for Nanomaterials, Advanced Technologies and Innovation, Technical University of Liberec, Studentska 1402/2, Liberec 1, Czech Republic, (e-mail: darina.jasikova@tul.cz).

imposing an intensive acoustic field into the bulk of liquid [1]. The acoustic field causes the local tension of the liquid and its rupture. Energy deposition represents another possibility for the bubble generation. The high density energy source can be laser radiation or an electric arc. The high energy plasma causes the local evaporation of the liquid and bubble creation. The bubbles created by the energy deposition can be generated either by electric discharge or the optical breakdown.

The optical breakdown in liquid is usually produced by focusing of the laser light through suitably designed optics. The laser induced breakdown in aqueous media and its collateral effects are described in detail by Kennedy in [2]. The energy distribution during the growth and collapse of laser induced bubble was described e.g. by Vogel in [3] and [4]. The authors investigated the influence of the laser pulse duration and input laser energy on the bubble dynamics and the shock waves emission.

The behavior of cavitation bubbles in water and isooctane generated by laser was investigated by Muller [5]. The generation of cavitation bubble is the most delicate part of the each experimental setup as the bubble must be spherical and undisturbed. Bosset [6] and Obreschkow [7] tested several optical assemblies for the generation of laser induced at 532 nm.

The most spherical bubble shape exhibited with the assembly using concave mirror for the laser beam focusing. The laser beam was expanded before the focusing by Galilean beam expander. One difficulty connected with the generation of the laser induced bubble is the limitation of its maximum size. The laser induced bubbles are usually produced in range of millimeters; however this requires high speed techniques for the bubble dynamics record.

The bubble dynamics response in the field of fluid can be detected acoustically by PVDF needle hydrophones or optically by high speed CCD cameras [8], [9]. The direct interaction between the cavitation bubble and the impact of its collateral effects can be detected by PVDF film sensors [8], [9]. These sensors are applicable in wide range of frequencies up to 1 MHz with very high sensitivity.

Here we try to understand the cavitation bubble behavior in a sense of observation its dynamics and visualize the types of the cavitation process with the most suitable technique. The aim of this work was to trace the relation between the output laser energy and the cavitation bubble size. This relation

depends also on the geometry of the optical devices that has to be correctly calculated and designed. In the following step we visualized the interaction of the cavitation bubble with the solid wall. This force interaction is dependent on the bubble size and the distance from the wall [10, 11 and 12].

In this paper we are not trying to set the physical statements and describe the background of the phenomenon both physically either mathematically, but the benefit of this research is to find the way in which the single cavitation bubble can be examined, visualized and valued.

Here we present results obtained with synchronized LIB, acoustic measurement, visualization for the state of the force interaction and the character of the cavitation bubble as well as process itself.

## II. PROBLEM FORMULATION

Here we are focused on the behavior of single bubble. For this purpose we select the optic cavitation as suitable method that enables to generate bubble spatially precisely and with defined diameter. [10] The liquid breakdown is caused by the local absorption of thermal and electromagnetic energy that leads to multi photon ionization followed with electron avalanche process, as visible plasma emission.

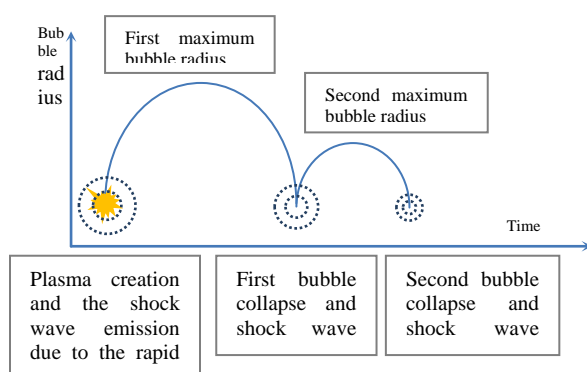


Fig. 1 the mechanism of cavitation bubble behavior in time

The term of optical breakdown is generally used for short pulse exposures. In our experiments we used the laser of pulse width 10ns. The laser induced breakdown (LIB) leads to plasma expansion that is followed by audible acoustic wave, supersonic velocities, shock waves and cavitation effects. [13]

The mechanism of the LIB is physically complex problem to be solved. The laser pulse generates the dense plasma of temperatures (6000 – 15000)K and pressures (20-60)kbar. This initial effect evokes bremsstrahlung emission and electron-ion recombination that can be noticed as visible flash in broadband light spectrum. The plasma expansion is followed by the shock wave and during this sequence the liquid is vaporized and a cavitation bubble is growing. This bubble is filled with water vapor. The bubble collapse occurs during the second phase of the bubble lifespan. The collapse is caused by the reduction of interior pressure and cooling that is influenced by the external environment.

This research was focused on the relation between the light

energy and the bubble size that can be produced in the experimental setup.

## III. LIB SETUP

For the single bubble generation we used here the setup for the laser induced breakdown (LIB).

The 10ns width laser pulse was generated using Q-switched Nd:YAG NewGemini pulse laser. This laser worked with one cavity for single shot generation on the wavelength 532nm. The outlet diameter of the laser beam was 5mm with Gaussian characteristics of intensity. In our research setup we used EFL1 - 75mm, and EFL2 - 300mm, magnification of 4times. This setup is followed with the golden mirror of the focus 50mm. The focused laser beam created the laser point (radius<0.1mm). Due the losses in the optical path on each of optical elements, comparable to this, we had to increase the energy level that enters the whole system. The set output energy of the laser is taken in account in the relation to the bubble diameter.

The diameter of the laser beam was 5mm. the magnification of the Galilean beam expander was calculated according to

$$MP = \frac{EFL_2}{|EFL_1|}. \quad (1)$$

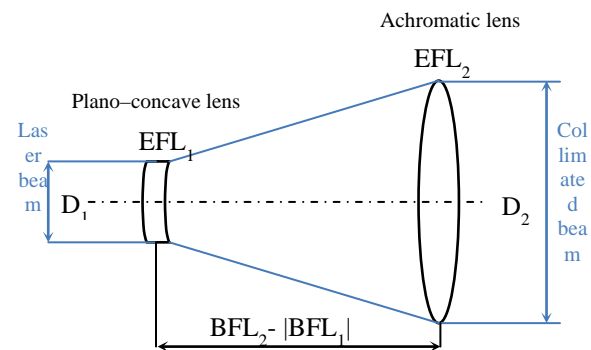


Fig. 2 the schema of the Galilean beam expander

## IV. VISUALIZATION SETUP

We used here the shadowgraphy setup for the bubble visualization. This setup consists of the 1.5kWatt continuous daylight lamp of light temperature 5200K and 110klux in the distance 1m far from the investigated object. The surrounded air was cooled with the ventilation system.

In the central horizontal axis, opposite to the light source was placed high speed CMOS camera SpeedSense from DantecDynamics. This camera is working on frequency 180kHz with resolution of (128x128)px or lower frequency with higher resolution up to (1280x800)px, and the dynamic range 12bit. The camera exposure time was 1μs. The sub-pixel resolution was 20μm.

The camera was mounted with optical lens system Nikon Macro 200 to get detailed image of magnification 1:1 in the distance 500mm far from the bubble. This setup ensured us optimal resolution and magnification of the image, so the pictures of the cavitation bubbles are contrast and detailed.

The camera was mounted with the 570nm low pass optical filter to reduce the backward laser flashes to the camera and also to eliminate the flash generated while plasmatic breakdown.

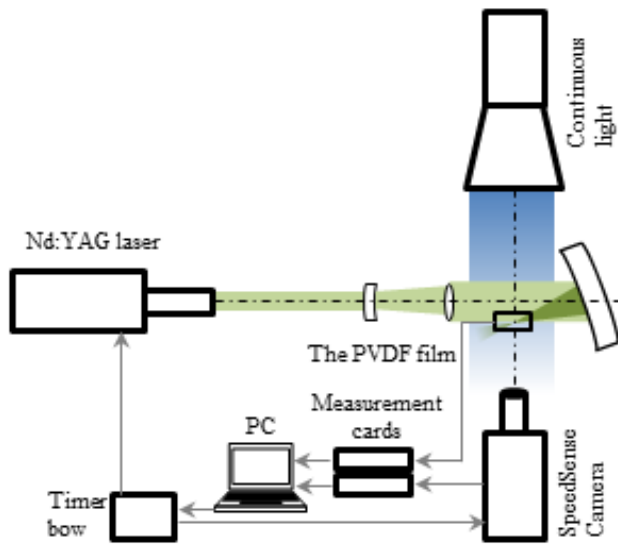


Fig. 3 the schema of the experimental setup of the LIB and visualization technique

#### V. PVDF FILM FORCE MEASUREMENT

The pressure response of the cavitation bubble was measured with PVDF film sensor DT1-028K W/TH (Measurement Specialties) in the far field. This sensor was also used to record the impact force from the bubble generated close to the wall. The signal from the PVDF film sensor was digitalized with the oscilloscopic card with the sampling frequency 60MHz. The PVDF film sensor was calibrated with the drop ball test and the measured calibration constant was 7.48mV/N.

The whole system (bubble generation, visualization setup and force measurement) was synchronized with the laser shot. The synchronization via the timer box was directly connected to the measurements cards in the computer. The signals were processed separately. The camera records were processed in Phantom Multi cam.

The investigation was realized with the water tank made from optical glass and filled with distilled water. We measured the parameters of water before and after the set of experiments and the values were following: the degree of dissolved air in the water 8.43mg/l and the conductivity 1.3 $\mu$ S/m. The degree of dissolved air gave us information for further comparable study of the dependence of cavity bubble characteristics on the degree of dissolved air. And the conductivity signifies the degree of impurities in water.

#### VI. RESULTS

For the relation between input laser energy and the bubble size that was generated with our optical setup, we create the dataset of size – measurement.

The energy of the laser beam was set and measured with

Ophir pyroelectric energy sensor. The dataset of at least 20 cavitation processes for statistic evaluation was captured. This maximum bubble size was detected in each image and it was related to the energy of the laser beam. The bubble size was measured in vertical and horizontal axis and the final value represents the average value. The increase of the laser energy causes the increase the horizontal value of the cavitation bubble size. This effect corresponds with the temporal and spatial plasma evolution at the very beginning of the process.

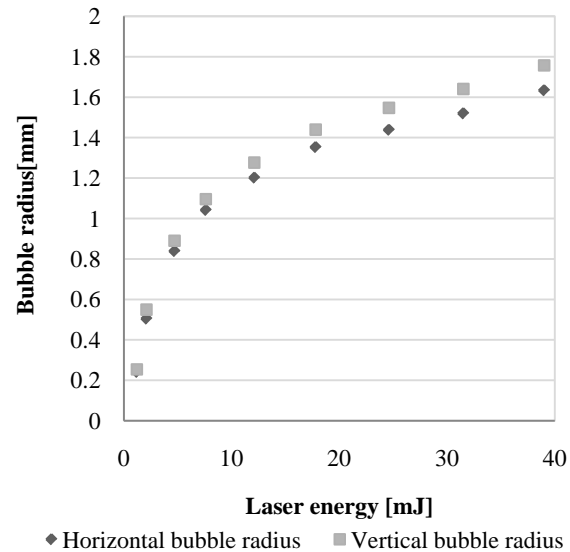


Fig. 4 the graph of the relation between the cavitation bubble radius and the input laser energy

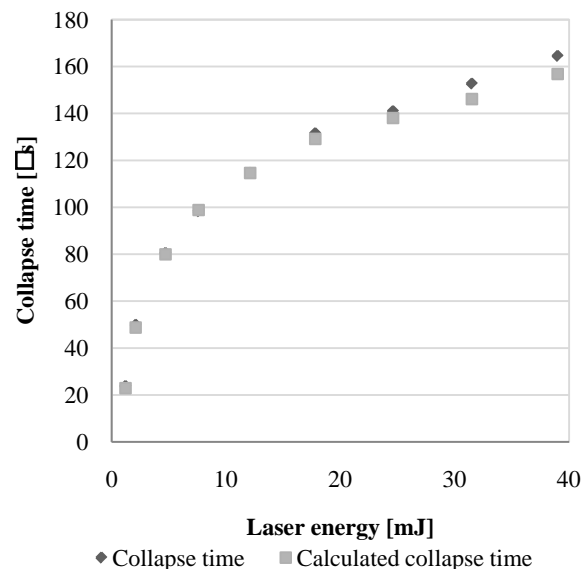


Fig. 5 the graph of relation between the bubble collapse time and the input laser energy

The relation between the energy of the laser beam and the cavitation bubble size is asymptotic. This means that further increase of laser energy does not lead to significant increase of the bubble size.

According to Kennedy [13], the plasma temperature shows asymptotic dependence on the laser pulse energy as well. With higher laser energy we recognized the negative influence of impurities and presence of segmentations on the bubble surface.

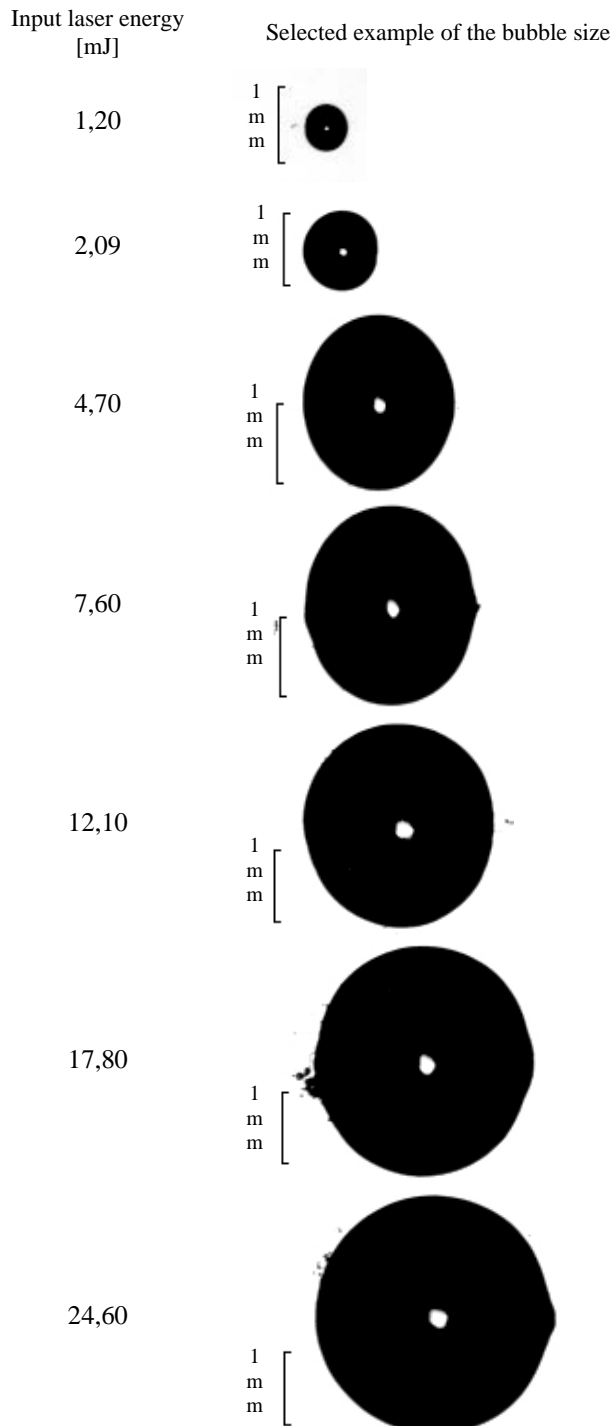


Fig. 6 the characteristic bubble shape for set input laser energy.

The process of LIB is not only characterized with the relation between the energy of the laser beam and cavitation bubble size, but also with the bubble dynamics. Rayleigh

(1917) expressed the quotation that represent the collapse time of the bubble (2).

$$t_c = 0.915 \sqrt{\frac{\rho_l R^2}{p_l - p_v}} \quad (2)$$

, where the  $\rho_l$  is the liquid density,  $R$  the radius of the bubble,  $p_l$  the atmospheric pressure in the surrounding liquid –  $10^5$ Pa and the  $p_v$  is the vapor partial pressure 2339Pa for 20°C.

The calculation of collapse time gives us important information and prediction about the bubble growth and dynamics. This is useful for the final experimental setup of the sample frequency of the camera and how long the process takes. As it is seen in Fig.5 collapse time is dependent on the cavitation bubble size, and finally on the input energy of the laser beam.

As we have successfully made the calibration pattern that gave us relation between the cavitation bubble size and the input laser energy (Fig. 4), we could follow in our research that is mainly focused on the impact of the cavitation bubble on the surface. With our experimental setup we got the very precise equipment that enables the generation of the cavity bubbles time, geometrically and spatial defined (Fig. 6).

In this part of experimental work we completed the experimental setup mentioned above with the PVDF film sensor attached to the wall. In the previous tests [7] that were based on single spark-generated cavitation, there were compared the results from the hydrophone and PVDF film. The signal correspondence between these two methods and the comparison of the measured pressure and force assured us in the good agreement.

The collapse pater that was detected synchronously showed the same trend and the peak of maximal and minimal values were temporary fitted.

Here in this measurement we were more interested in the impact force from the bubble on the wall. We worked with the input laser energy 4.7mJ that led to the generation of the symmetrical regular shape bubble radius of size 0.83mm.

We run the serial of experiments varying in the distance of the bubble and the wall. The crucial distances were: the whole diameter, half of the diameter, half of the radius and the edge of the bubble.

Here we present the results taken in two interesting distances i.e. the two whole diameters and the bubble radius. The force measurement is related to the visualization.

The images were captures in the resolution (128x184)px with the frequency 130.232 kHz. The starting point of the measurement is the shot from the laser that initiates the breakdown. The plasmatic flash can be sometimes seen on the firs image.

Two PVDF film signals corresponding to two bubble wall distances are presented in the Fig. 7 and Fig. 8. The first peak in the signal at Fig. 7 (up to 5  $\mu$ s) corresponds to the interaction between the wall and shock wave, which is radiated at the bubble initiation due to rapid plasma expansion. After this phase the bubble starts to expand up to the first maximum radius, which is reached about 51 $\mu$ s.

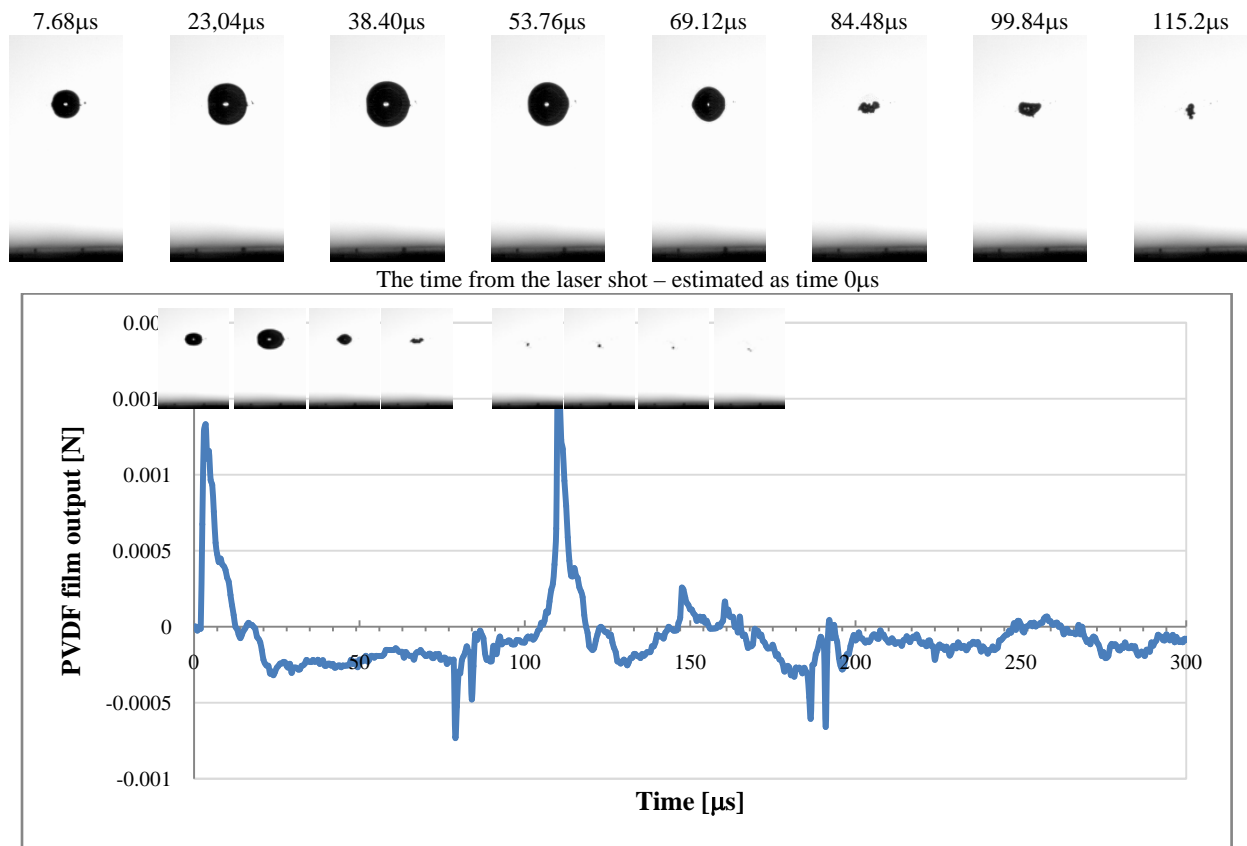


Fig. 7 the visualization of single cavitation bubble development in selected time steps and the synchronized force measurement

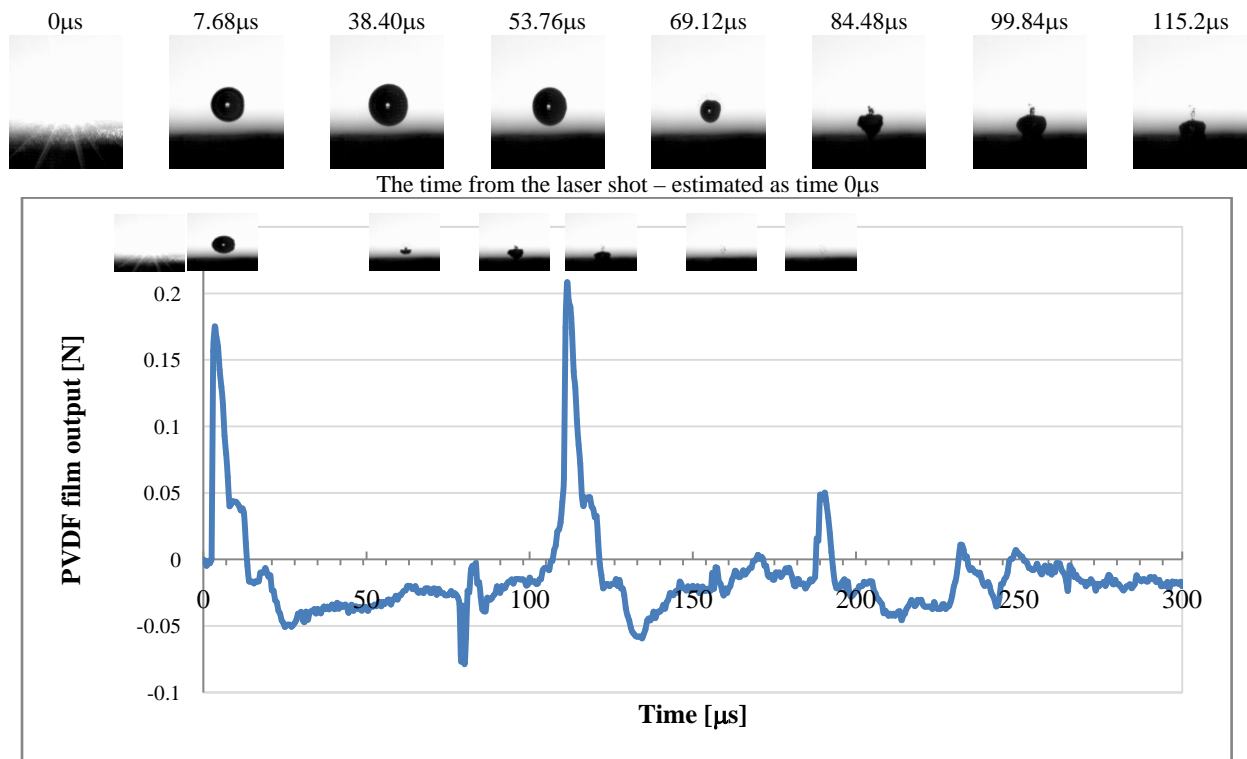


Fig. 8 the visualization of single cavitation bubble development in selected time steps and the synchronized force measurement

Then the bubble starts to collapse. The final stage of the collapse is associated with the shock wave production, which can be identified at the signal by the peak about 109 $\mu$ s.

After this phase the bubble expand to the second maximum radius followed by second bubble collapse. The shock wave generated during the second collapse can be identified at the signal about 143 $\mu$ s. In this position the bubble wall interaction is realized only due to shock waves. The first peak in the signal at Fig. 8 (up to 5 $\mu$ s) corresponds to the interaction between the wall and shock wave. Then the bubble expands to the first maximum radius followed by first collapse represented by peak at 110 $\mu$ s. In contrast to previous case the bubble is during the final state of the collapse attracted to the wall. This movement continues during the second bubble expansion. The second bubble collapse proceeds already at the wall, which can be identified by the peak about 180 $\mu$ s.

The experimental setup of the LIB enables us the precisely set the spatial geometry of the cavitation bubble generation. The further study followed the trend of the impact force on the various surfaces and the character of the shape in the implosion phase. The shape of the implosion phase of the cavitation bubble corresponds directly to the impact force that was measured on the wall surface.

Anyway as the bubble lifespan can be divided into two phase, the visualization was also studied separately.

During the first phase the bubble grows and expands and the distance to the surface was estimated from the maximum bubble size. In the second phase of the bubble implosion, there is visible the significant influence of the bubble distance.

Time after LIB:  
7,68 $\mu$ s   15,36   23,04   30,72   38,4   46,08   53,76   61,44  
 $\mu$ s    $\mu$ s

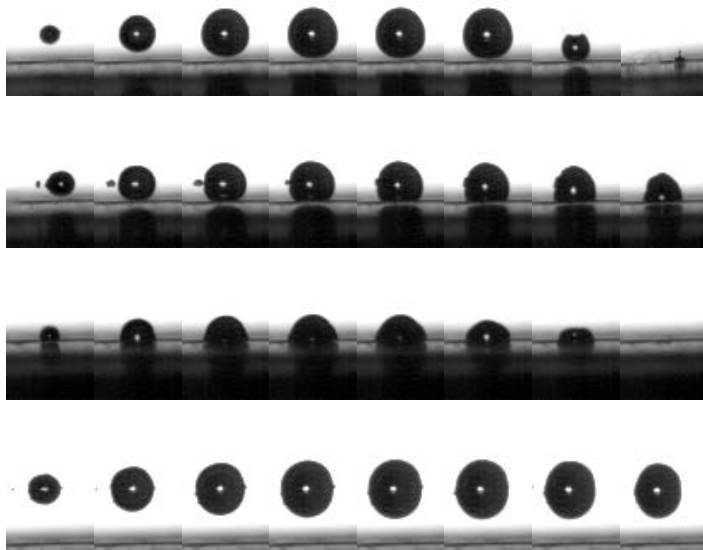


Fig. 9 first part of cavitation bubble lifespan- the growth of the bubble and the start of the implosion

Figure 9 shows the cavitation bubble in the first part of grows in four distances to the surface. The first row presents

the bubble generated in the distance equal to the bubble diameter, the second row the distance to the half of maximum bubble diameter; the third row the half of the bubble radius and the fourth row represents the bubble generated in the distance one and half diameter to the surface. Already in this stage there is seen small force impact on the surface, especially when the bubble is generated close enough to the surface or is directly detached. It is obvious that the detached bubbles have the major influence on the damages of the surface. There is mentioned in the introduction part that probability of the cavitation bubble raise increase with the impurities in the water so there is the no striking information that those impurities are mostly present on the surfaces so there is further increase of the damage.

As it is seen this phase is crucial for the further behavior of the single bubble. In the second phase, during the implosion and the bubble destruction the force impact is raised and it is visible that the impact force is growing also with the distant bubbles. The figure 10 corresponds with the figure 9 and the rows are following.

Time after LIB:  
69,12   76,8   84,48   92,16   99,84   107,52   115,2   122,88  
 $\mu$ s    $\mu$ s

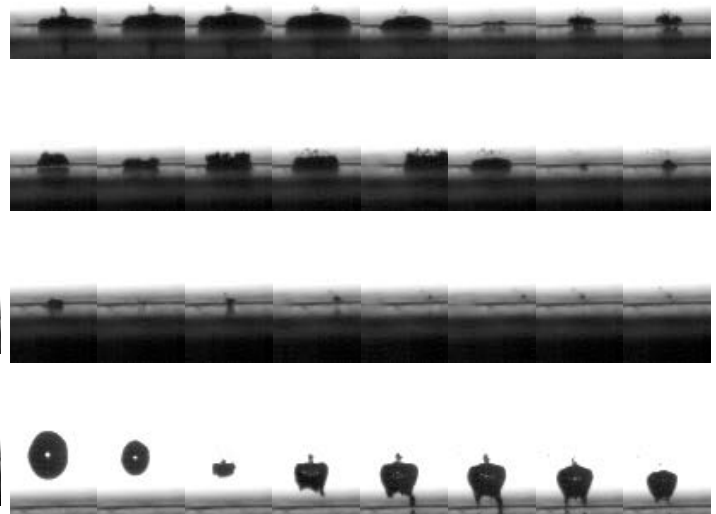


Fig. 10 second part of cavitation bubble lifespan – the implosion with the wall impact geometry

## VII. CONCLUSION

The main goal of this research was to set the optical setup for the laser induced breakdown and to create the calibration relation curve for the bubble size dependence on the input energy of the laser beam.

This calibration curve was related to the collapse time of the cavitation bubble to estimate the lifespan of each bubble. This information was the entry condition for the setup of the visualization technique.

Here we used the high speed shadowgraphy setup. The

visualization was synchronized with the pressure response measured with PVDF film sensor attached to the solid wall. The interaction between the cavitation bubbles was studied with both techniques: the valuated visualization and the signal from the PVDF film.

Time evolution of the PVDF film signal has the same characteristics but maximum and minimum peak values are influenced by the distance between the bubble and the wall position.

As we are dealing with powerful experimental technique that enables the generation of single highly defined cavitation bubble in time and space, the following research will be focused on the impact of the cavitation bubble force on the elastic wall and the measurement of the temperature field in the bubble surroundings. The next step is the estimation of cavitation bubble characteristics on the degree on the dissolved air and the level of impurities in the water.

#### REFERENCES

- [1] W. Lauterborn, T. Kurz, R. Mettin, P. Koch, D. Kroninger, D. Schanz, "Acoustic cavitation and bubble dynamics", *Archives of Acoustics*, Vol. 33, pp. 609-617, 2008.
- [2] P. Kennedy, D. Hammer, X. Daniel, "Laser-induced breakdown in aqueous media", *Progress in Quantum Electronics*, Vol. 21, No. 3, pp. 155-248, 1997.
- [3] A. Vogel, S. Busch, U. Parlitz, "Shock wave emission and cavitation bubble generation by picosecond and nanosecond optical breakdown in water", *J. Acoust. Soc. Am.*, Vol. 100, No. 1, pp.148-165, 1996.
- [4] A. Vogel, et al., "Energy balance of optical breakdown in water atononosecond to femtosecond time scales", *Applied Physics B: Lasers and Optics*, Vol. 68, pp. 271-280, 1999.
- [5] M. Müller, W. Garen, S. Koch, F. Marsik, W. Neu, E. Saburov, "Shock Waves and Cavitation Bubbles in Water and Isooctane generated by Nd:YAG Laser", *Experimental and Theoretical Results, Proc. SPIE*, Vol. 5399, pp. 275-282, 2004.
- [6] A. De-Bosset, D. Obreschkow, P. Kobel, N. Dorsaz, M. Farhat, "Direct effects of gravity on cavitation bubble collapse", *Proceedings of the 58 international astronomical congress*, pp. 1-5, 2007.
- [7] D. Obreschkow, M. Tinguely, N. Dorsaz, P. Kobel, A. De Bosset, M. Farhat, "The quest for the most spherical bubble: experimental setup and data overview", *Experiments in Fluids*, Vol 54, pp.1503, 2013.
- [8] Yi-Chun Wang, Yu-Wen Chen, "Application of piezoelectric PVDF film to the measurement of impulsive forces generated by cavitation bubble collapse near a solid boundary", *Experimental Thermal and Fluid Science*, Vol. 32, pp. 403-414, 2007.
- [9] W. Lauterborn, "Optic cavitation", *Journal de physique*, Vol 11, No. 40, pp. 273-278, 1979.
- [10] L. A. Maglaras, "The influence of the effect of grounding and corona current to the field strength the corona onset and the breakdown voltage of small air gaps", *Wseas transactions of power systems*, Vol. 3, pp. 103-110, 2008.
- [11] F. Della Torre, "Dynamic analysis of electric arc: from the single-phase state approach to the three-phase Clarke approach", *Wseas transactions of power systems*, Vol. 3, pp. 90-94, 2008.
- [12] G.Kil, "Analysis of partial discharge in insulation oil using acoustic signal detection method", *Wseas transactions of power systems*, Vol. 3, pp. 436-445, 2008.
- [13] P. K. Kennedy et al., "Laser-induced breakdown in aqueous media", *Prog. Quant. Electr.*, Vol. 21, No. 3, pp. 155-248, 1997.